

7.10 The Magnetic Cavern of L3

Alain Hervé

The L3 detector was designed to measure with unprecedented accuracy and resolution electrons, photons and muons produced in the particle collisions. These particles passed through a sequence of detector systems where they were tracked and identified according to their characteristic signatures: the vertex-chamber, the electromagnetic calorimeter, the hadronic calorimeter and the muon chambers. This mission called for a highly specific architecture of the detector, in particular the experimental hall, the unconventional magnet, the muon system and the support of the system of inner detectors surrounding the beam pipe at the collision point [24] (see Fig. 7.21).

The original idea was to integrate the magnet yoke into the rock of the cavern, whence the name “magnetic cavern” which would stay with L3. Finally, it was decided for ease of maintenance of the muon chambers and to access equipment with a travelling crane to increase the size of the cavern. The 21.4 m diameter, 26.5 m long experimental hall is oriented longitudinally along the LEP beam line that enters the hall with a slope of 1.39%: the complete detector is inclined to follow this slope. A 23 m diameter and 52 m deep access shaft connects to one end of the experimental hall, for installing experimental equipment. After the installation of the major large components the shaft was used for the installation of experimental services (water, cables, gas, ventilation, etc.), and as technical space for installing power converters, cryogenics, monitoring equipment and offices.

Observing muons with state-of-the-art momentum resolution was one of the L3 priorities: an important ingredient was the largest magnet ever built for a particle physics experiment. The octagonal shaped magnet has a yoke consisting of 6400 t of low carbon steel and an 1100 t aluminum coil. Given the size of the coil, it was built from individual octagonal aluminum sections, each one being built at CERN. These sections were subsequently integrated into the yoke. A current of thirty thousand amperes in the aluminum coil generated a uniform field of 0.5 T. The magnetic circuit of the octagonal yoke had to be closed with massive iron endplates. These endplates, each weighing 700 t, were split in the middle and could be opened like doors to give access to the muon detectors for maintenance. The magnet is lined with an active thermal screen providing a thermally controlled environment to the particle detectors. The yoke rests on a concrete cradle integrated in the floor of the detector hall.

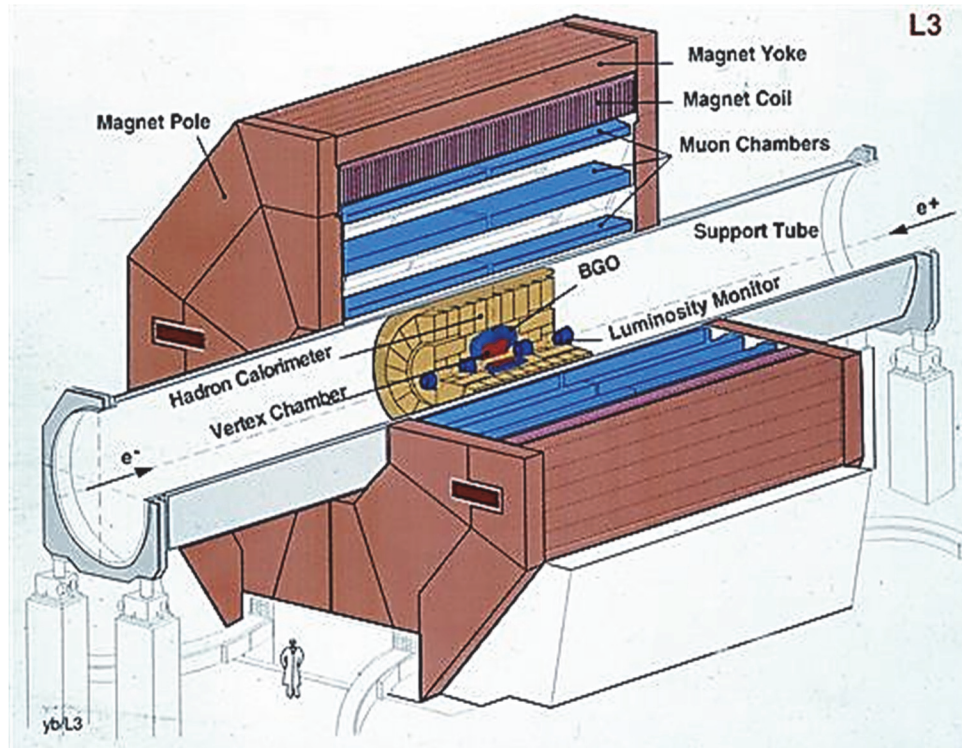


Fig. 7.21. Overview of the L3 detector [24].

Inside the magnet precision Muon Chambers were arranged in three concentric layers, to measure the trajectories of muons in the magnetic field over a volume of 1000 m^3 . To achieve the design momentum resolution these chambers were built with mechanical tolerances of $30 \mu\text{m}$ over an area of $3 \text{ m} \times 6 \text{ m}$. Sixteen octants of muon chambers were supported on two support tubes. Several precision straightness monitors, using LEDs and quadrant photodiodes were specially developed to ensure accurate mutual alignment of the chambers within an octant. At the time this muon system was the most advanced of its kind: its success encouraged the LHC collaboration ATLAS to adopt the concept and take it to the next level of dimension and performance [Highlight 8.12].

The 300 t support tube, 30 m long and 4.45 m in diameter was another rather daring innovation that contributed to the performance of the muon spectrometer. It passed through the magnet coaxial with the beam line. It rested on continuously adjustable servo-controlled jacks placed on concrete pillars. The part of the support tube inside the magnet was of non-magnetic stainless steel, the remaining portion in carbon steel. In this way the support tube rendered all detector systems (600 t in total) mechanically independent of the magnet.

The hadron calorimeter measured the energy of elementary particles, jets of particles, and contributed to muon identification [Box 3.2]. It consisted of 300 t of depleted uranium plates sandwiched between some 8000 proportional chambers.

The electromagnetic calorimeter was another “world première”, designed to measure the energies and positions of electrons and photons from 100 MeV to 100 GeV with high resolution [Highlight 7.9].

Charged particles were tracked in the time expansion chamber which had to be of limited radius to fit inside the BGO calorimeter. It featured an interesting variant of the MWPC [Highlight 4.8] measuring tracks with 40 μm accuracy in a volume of one cubic metre. At the beginning of 1991, the radius of the LEP beam pipe was reduced from 8.0 cm to 5.5 cm. L3 took advantage of this extra space by installing a Silicon Microstrip Detector (SMD) to upgrade its central tracking capability.

The L3 experiment was an important precursor to the LHC experiments. The precision crystal electromagnetic calorimeter was a precursor of the CMS electromagnetic calorimeter [Highlight 8.8]. The alignment of muon chambers using optical systems was further developed for the ATLAS muon spectrometer.

L3 was the only LEP experiment installed stationary at the interaction point (as is the now case for the LHC experiments). The other LEP experiments were assembled adjacent to the accelerator, to be pulled in and out on rails so that LEP could continue to be operated if an experiment required extensive maintenance. New procedures for installation and maintenance had to be developed to take into account the interaction with the machine. To gain time in the installation sequence, heavy parts of the detector, such as the support tube and the hadron calorimeter barrel (weighing each around 300 t) were completed in the surface hall prior to installation in the cavern using rented heavy lifting equipment. Following this experience, the same technique was used extensively for the CMS experiment.

The L3 experimental area and large magnet has been reused to house the ALICE LHC experiment. This was a magnificent legacy, allowing L3 infrastructure to be re-used, in true CERN fashion, for ALICE, a state-of-the-art experiment dedicated to the study of heavy ion collisions at the highest possible energy.

References

1. B. Richter, Very high energy electron-positron colliding beams for the study of the weak Interactions, *Nucl. Instr. & Meth.* **136**, 47 (1976), and SLAC-PUB-1738.
2. C. Pellegrini, C. Rubbia and A. Ruggiero, Comments on the desirability and feasibility study for e^+e^- colliding rings with $L = 10^{32} \text{ s}^{-1}\text{s}^{-2}$ and $E_{\text{cm}} = 120 \text{ GeV}$, CERN-NP Int. Rep. 75-11 (1975). <https://cds.cern.ch/record/1161844?ln=en>.
3. LEP Summer Study, Les Houches, France and CERN, Sept. 1978, CERN-79-01-V-2, (1979). <https://cds.cern.ch/record/133077?ln=en>.

4. A. Zichichi (Ed.), ECFA-LEP Working Group report (“The white book”) ECFA 79/79 (1980), reproduced in <https://cds.cern.ch/record/816523?ln=en>.
5. M. Bourquin (Ed.), General meeting on LEP, Villars, ECFA-91-054 (1981). <https://cds.cern.ch/record/98884?ln=en>.
T. Ekelof and G. Flugge (Eds.), International conference on experimentation at LEP, Uppsala, *Physica Scripta* **23** 4 1 & 2 (1981).
6. J. Adams, CERN Annual Report 1980, p. 25 (1981). <https://cds.cern.ch/record/1475744?ln=en>.
7. J. Ellis and R. Peccei (eds.), *LEP Physics Jamboree - LEP Exp. Committee*, CERN-1986-002 (CERN, Geneva, 1986). <http://dx.doi.org/10.5170/CERN-1986-002>.
8. K. Johnsen *et al.* (eds.), *Design Concept for a 100 GeV e^+e^- Storage Ring (LEP)*, CERN-1977-014 (CERN, Geneva, 1977). <http://dx.doi.org/10.5170/CERN-1977-014>;
LEP Study Group, *Design Study of a 15 – 100 GeV e^+e^- Colliding Beam Machine (LEP)*, “Blue Book”, ISR-LEP 78/17 (CERN, Geneva, 1978). <https://cds.cern.ch/record/101331>;
LEP Study Group, *Design Study of a 22 – 130 GeV e^+e^- Colliding Beam Machine (LEP)*, “Pink Book”, ISR-LEP 79/33 (CERN, Geneva, 1979). <https://cds.cern.ch/record/101333>.
9. CERN, LEP phase 1 and cost breakdown, CERN/SPC/0472, (1981), <https://cds.cern.ch/record/61975?ln=en>.
10. CERN, Etude d’impact du projet LEP sur l’environnement, (1982). <https://cds.cern.ch/record/99730?ln=en>.
11. LEP design report (“The green book”), Vol. II, The LEP main ring, CERN-LEP/84-01 (1984). <http://cds.cern.ch/record/102083?ln=en>.
12. H. Laporte, La construction du LEP, *Revue Travaux (Science et Industrie)*, Paris (1988).
13. G. Bachy *et al.*, The LEP collider: construction, project status and outlook, *Particle Accelerators*, **26**, pp. 19-32 (1990).
14. H. Schopper, *LEP, Lord of the Collider Rings at CERN* (Springer, Berlin, 2009).
15. E. Picasso, LEP construction, (2009). <https://cds.cern.ch/record/1228538?ln=Fr>.
E. Picasso, A few memories from the days at LEP, *Eur.Phys.J.* **H36** pp. 551-562 (2012)
DOI: 10.1140/epjh/e2011-20050-0.
16. K. Hubner, Designing and building LEP, *Physics Reports* **403-404**, 177-188 (2004);
S. Myers (ed.), *The LEP Collider: from Design to Approval and Commissioning*, CERN-1991-008 (CERN, Geneva, 1991). <http://dx.doi.org/10.5170/CERN-1991-008>.
17. C. Wyss (Ed.) LEP design report, Vol. III, LEP2, CERN-AC-96-01-LEP-2 (1996). <http://cds.cern.ch/record/314187?ln=en>.
18. LEP design report, Vol. I, The LEP injector chain, CERN-LEP-TH-83-29 (1983). <http://cds.cern.ch/record/98881?ln=en>.
19. T. Taylor, Technological aspects of the LEP low-beta insertions, *IEEE NS-32* (1985).
20. P. Bernard, Superconducting RF cavities, *Lectures in honour of E. Picasso*, Pisa (1999), CERN-OPEN-2010-001. <https://cds.cern.ch/record/1231370?ln=de>.
21. ALEPH, *Nucl. Instr. & Meth. A*, **294**, 121-178 (1990), *Nucl. Instr. & Meth. A*, **303**, 393 (1991), CERN-EP-90-2
22. DELPHI, *Nucl. Instr. & Meth. A*, **303**, 233-276 (1991), CERN-PPE-90-128, CERN- EF-90-5.
23. OPAL, *Nucl. Instr. & Meth. A*, **305**, 275-319 (1991), CERN-PPE-90-114.
24. B. Adeva *et al.*, The construction of the L3 experiment, *Nucl. Instr. & Meth. A* **289**, pp. 35–102 (1990).
25. ADLO Collaborations, Lower bound for the Standard Model Higgs boson mass from combining the results of the four LEP experiments, CERN-EP/98-046 (1998).

26. ADLO Collaborations *et al.*, Precision ElectroWeak measurements on the Z resonance, *Physics Reports*, **427**, 257-454 (2006).
27. D. Treille, LEP/SLC: What did we expect? What did we achieve? A very quick historical review, *Nucl. Phys. Proc. Suppl.* **109 B** 1-16 (2002).
28. G. Altarelli (ed.), *Workshop on Physics at LEP2*, CERN-1996-001-V-1 (CERN, Geneva, 1996). <http://dx.doi.org/10.5170/CERN-1996-001-V-1>.
29. J.P. Gourber and C. Wyss, Prototypes of LEP bending magnets with steel-concrete cores, *IEEE Trans. Nucl. Sci.* **NS-28**, 3, 2867 (1981).
30. L. Resegotti, The LEP magnet system, (*MT-8*), *J. Phys. Colloques*, **45**, C1-233-C1-239 (1984).
31. J. Billan, J.P. Gourber and K.N. Henrichsen, Geometry and remanent field measurement of the LEP dipole magnets, (*MT-8*), *J. Phys. Colloques*, **45**, C1-953-C1-956 (1984).
32. LEP-Vacuum Group, LEP vacuum system: present status, *Proc. 11th Int. Vacuum Congress*, Köln, Germany (1989).
33. C. Benvenuti and F. Francia, Room temperature pumping characteristics of a Zr-Al Non-Evaporable Getter (NEG), *J. Vac. Sci. Technol.* **A6**, 2528 (1988).
34. C. Benvenuti and F. Francia, Room temperature pumping characteristics for gas mixtures of a Zr-Al nonevaporable getter, *J. Vac. Sci. Technol.* **A6**, 3864 (1990).
35. C. Benvenuti, N. Circelli and M. Hauer, Niobium films for superconducting accelerating cavities, *Appl. Phys. Lett.* **45** (5) p. 583 (1984).
36. C. Benvenuti *et al.*, Preparation of niobium coated superconducting RF cavities for the Large Electron Positron Collider, *Proc. III workshop on RF Supercond.*, **ANL-PHY-88**, 445 (1988).
37. A. Butterworth *et al.*, The LEP superconducting RF system, *Nucl. Instr. & Meth. A*, **587**, 151–177 (2008), and E. Jensen, RF cavity design, CAS 2013, Trondheim, <https://cds.cern.ch/record/1982429/files/arXiv:1601.05230.pdf>
38. The LNN-INFN international workshop on thin films, LNL Laboratories, Padova (2006).
39. S. Turner, (ed.), *Lecture Notes in Earth Sciences n°12*, pp. 207-394 (Springer, Berlin, 1986).
40. G. Beutler and W. Gurtner, Test of GPS on the CERN-LEP Control Network, *Schriftenreihe der Universität der Bundeswehr München, Heft 20-2*, pp. 337–385, (1985).
41. J. Gervaise and M. Mayoud, in *Advances of Accelerator Physics and Technologies*, (World Scientific, Singapore, 1993), pp. 546–584.
42. M. Mayoud, in *Frontiers of Accelerator Technology*, (World Scientific, 1996), pp. 717–742.
43. L. Arnaudon *et al.*, Effects of terrestrial tides on the LEP beam energy, *Nucl. Instr. & Meth. A*, **357**, 249, (1995).
44. B. Mours *et al.*, The Design, construction and performance of the ALEPH silicon vertex detector, *Nucl. Instr. & Meth. A* **379**, pp.101–115 (1996).
45. V. Chabaud *et al.*, The DELPHI silicon strip microvertex detector with double sided readout, *Nucl. Instr. & Meth. A* **368**, pp. 314–332 (1996).
46. K.H. Becks *et al.*, The DELPHI pixels, *Nucl. Instr. & Meth. A* **386**, pp. 11–17 (1997).
47. M. Acciarri *et al.* (for the L3 SMD Collaboration), The L3 silicon microvertex detector, *Nucl. Instr. & Meth. A* **360**, 103–109 (1995).
48. S. Anderson *et al.* (for the OPAL Collaboration), The extended OPAL silicon strip microvertex detector, *Nucl. Instr. & Meth. A* **403**, pp. 326–350 (1998).
49. K. Abe *et al.*, Design and performance of the SLD vertex detector, a 307 Mpixel tracking system *Nucl. Instr. & Meth. A* **400**, pp. 287–343 (1997).
50. J. Seguinot and T. Ypsilantis, Photoionization and Cherenkov ring imaging, *Nucl. Instr. & Meth.* **142**, p. 377 (1977).

51. T. Ekelof, J. Seguinot, J. Tocqueville and T. Ypsilantis, The Cherenkov Ring-Imaging Detector: Recent Progress analysis and Future Development, *Physica Scripta* **23**, 718 (1981).
52. W. Adam *et al.*, The Ring imaging Cherenkov detector of DELPHI, *Nucl. Instr. & Meth. A* **343**, pp. 68–73 (1994).
53. W. Adam *et al.*, Performance of the forward RICH detector system at DELPHI, *Nuclear Science* **4**, No. 3, 583 (1993).
54. P. Baillon *et al.*, An improved method for manufacturing accurate and cheap glass parabolic mirrors, *Nucl. Instr. & Meth. A* **276**, 492 (1989).
55. P. Baillon *et al.*, Production of 300 paraboloidal mirrors with high reflectivity for use in the barrel RICH counter in DELPHI at LEP, *Nucl. Instr. & Meth. A* **277**, 338 (1989).
56. P. Baillon *et al.*, Gamma ray spectrum of the Crab nebula in the multi TeV region, *Astroparticle Physics* **1**, p. 341 (1993).
57. M.J. Weber and R.R. Monchamp, Luminescence of Bi₄Ge₃O₁₂: spectral and decay properties, *J. Appl. Phys.* **44**, p 5495 (1973).
58. E. Lorenz, Status of BGO development and perspectives of BGO calorimeters in high energy physics, *Nucl. Instr. & Meth. A* **225**, p. 500 (1984).